# DFT study on the structure and stability of $TeO_2$, $TeO_4$ and $Te(OH)_4$ crystals

Bohnni Shikha Biswas,* Cornelio Mariano Cap López,† and Raman D K‡
*Online students*
*Computational Materials Physics*
(Dated: December 12, 2021)

## I. INTRODUCTION

Polonium-$_{84}Po^{209}$ is a radioactive element discovered by Mme. Curie in 1898 [1]. This radioactive property is a boon and as well as a curse. Polonium was used as a power resource in the Soviet's Luna spacecraft [2]. It is alloyed with Beryllium for generating neutrons [3]. But all Polonium isotopes radioactive and unstable. Out of these, only $_{84}Po^{210}$ occurs naturally [4]. This makes tedious to study their properties in normal conditions. The motive of this project is to facilitate the study of Polonium hydroxides. The hydroxides of Tellurium are a good candidate for studying similar polonium systems due to their resemblance in some periodic properties. Te and Po share the same oxidation states, and boiling point [5]. The formation energy, supercell structure and stability of $TeO_2$, $TeO_4$, and $Te(OH)_4$ are analysed in this paper.

## II. COMPUTATIONAL METHODS

### A. Methods

The cif files for $TeO_2$, Te and $O_2$ were obtained from the Materials-Project website[6]. All calculations for the crystals were carried out using the Quantum Espresso DFT code [7, 8] using Generalized Gradient Approximation (GGA) [9] with PBE exchange correlation functional [10] and plane wave pseudopotentials. Their relative molecular gas phase optimization was done using Gamess DFT code [11]. The gas phase DFT calculations were carried out using the 3-21G Gaussian type basis set with B3LYP exchange functional [12].

### B. Details

A series of Self Consistent Field (SCF) calculations on orthorhombic-$TeO_2$(id=mp2125)[6] were carried out, altering the k-mesh values, energy cut-off and its multiplication factor. The corresponding fluctuations in their hydrostatic pressure were studied. In this manner the convergence testing was done and a convincing k-mesh and basis set size was chosen. With the chosen parameters, another set of SCF calculations with altering lattice parameter-a by $\pm$ 0.04 Å was carried out. A graph was plotted with the lattice parameter against Energy and a lattice parameter corresponding to a minimum energy is obtained. A Birch-Murnaghan equation of state fit was generated to obtain the bulk modulus, equilibrium energy and volume. With the found volume, a full optimization was carried out using Quantum Espresso's vc-relax calculation with an isotropic target pressure of zero kilo-bar to find the minimum energy and volume. A similar optimization procedure was applied for Te(id=mp19) [6] crystal and $O_2$(id=mp12957) [6] supercell and the formation energy of $TeO_2$ was calculated. The cif2cell [13] tool was used for building the supercells of $O_2$, $TeO_4$, and $Te(OH)_4$. The hypothetical molecular crystals, $Te(OH)_4$ and $TeO_2$ were built using Vesta program [14] and FINDSYM [15, 16] was used to generate symmetry positions. The supercell size convergence tests were carried to find optimal supercell size and a full optimization of unit cell by using vc-relax scheme was done. The obtained energy was considered as the minimum energy of stable crystal structures of $TeO_4$ and $Te(OH)_4$. A typical optimization of these molecules in gaseous state were carried out using GAMESS DFT code [11]. The gaseous state energy and the supercell energy was compared and the stability of $TeO_4$ and $Te(OH)_4$ was realized.

## III. RESULTS

### A. Convergence Test

The first task of the project was to find the optimal set of parameters such as k-mesh size and energy cuts values; in order to have acceptable numerical results from the DFT calculations made with Quantum Espresso. Since no reference was used to perform this project, the first guess for the k-mesh sized was of $1 \times 1 \times 1$. Then several tests were performed chosing all the odd k-mesh size values from $3 \times 3 \times 3$ up to $11 \times 11 \times 11$, however, besides the coputational time, which took several minutes from the lowest k-mesh sizes up to hours with the highest sizes; no particular difference was found in the behaviour of the hydrostatic pressure values.
As an example, the hydrostatic pressure as function of the energy cut-off of the wave fucntion is shown in figure 1. This plot corresponds to a $3 \times 3 \times 3$ k-mesh size, here it can be seen that the pressure changes a lot from the

* biswasbohnni@gmail.com
† cmcap06@gmail.com
‡ raman.freak@protonmail.com

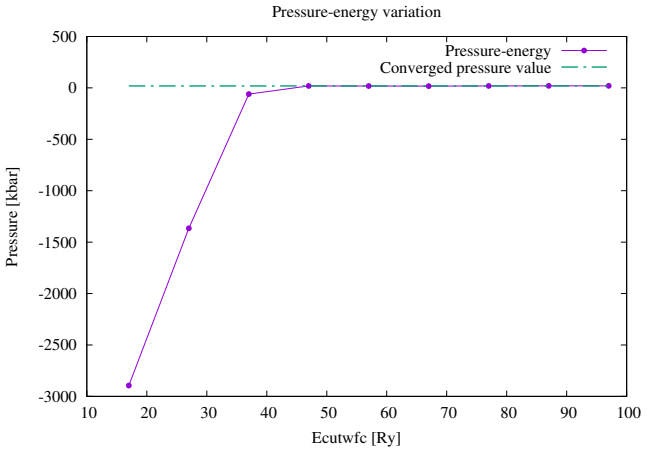


FIG. 1. Hydrostatic pressure variation as function of the energy cut-off of the wave function. The plot corresponds to a $3 \times 3 \times 3$ k-mesh size, the green dashed line represents the pressure convergence value around 19 kbar.

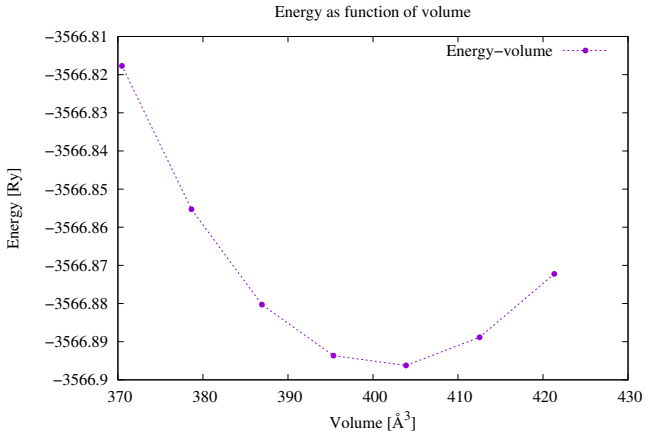


FIG. 2. Total energy as a function of volume variations. The minimal energy corresponds to the volume of 403.89 Å$^3$.

TABLE I. Rescaling of the size of the crystal and it's total energy.

| Lattice Parameter $a$ [Å] | Volume [Å$^3$] | Energy [Ry] |
|---|---|---|
| 5.71918 | 421.320033 | -3566.872227 |
| 5.67918 | 412.511569 | -3566.888839 |
| 5.63918 | 403.885889 | -3566.896232 |
| 5.59918 | 395.352153 | -3566.893651 |
| 5.55918 | 386.939468 | -3566.880280 |
| 5.55918 | 378.646976 | -3566.855267 |
| 5.47918 | 370.473817 | -3566.817692 |

lowest energy value and it starts to converge for energy cut-off bigger than 40 Ry. After doing the same analysis for the other k-mesh sizes values, a similar pattern was observed, and, the hydrostatic pessure convergence value always reached a value around 19 kbar. Therefore, taking into account a reasonable computational time for the calculations the k-mesh size of $3 \times 3 \times 3$ was choosed, with a wave function energy cut-off of 87 Ry and a density energy cut-off of 609 Ry.

### B. Geometry Optimization

With the right set of parameters, the next step was to calculate the optimized geometry of our $TeO_2$ crystal. For this, we rescaled the crystal size as explained in II B and performed a DFT calculations in order to obtain the total energy of the crystal. The results for this are shown in table I and ploted in figure 2. From the parabolic curve, it can be witnessed that it reaches a minimum value of the total energy at certain point corresponding to a volume of 403.8858 Å$^3$.

Using the *ev.x* tool as a first approximation, it was possible to calculate the equilibrium volume $V_0$, ground state energy $E_0$ and Bulk modulus $B_0$ by fitting the data to the Birch-Murnaghan equation of state [17, 18]. The results are shown in table II,

TABLE II. Values obtained for the Birch-Murnaghan equation of state using *ev.x* tool.

| Volume [Å$^3$] | Bulk modulus [GPa] | Energy [Ry] |
|---|---|---|
| 401.73 | 124.4 | -3566.89655 |

Finally, using the the volume of 403.89 Å$^3$ which corresponds to the minmal energy as shown in figure 2 and the set of parameters discussed in section III, we performed a vc-relax calculation, from which we obtained the results showing in table III

### C. Formation energies of $TeO_2$

The formation energy of $TeO_2$ is calculated by substracting its minimum energy from the sum the of the minimum energies of Te and $O_2$ . For this, Te(id=mp19) [6] unit cell is optimized and the minimum energy is obtained. For oxygen, a supercell is built and supercell size convergence is done. Table lists the energies of various cell sizes and among those, the $2\times2\times2$ supercell exists in

TABLE III. Physical quantities for the fully optimized $TeO_2$ crystal after the vc-relax calculation.

| Physical quantity | Calculated value |
|---|---|
| Total pressure | 0.02 GPa |
| Total energy | -3566.8976 Ry |
| Lattice parameter $a$ | 5.6392 Å |
| Volume | 396.3610 Å$^3$ |

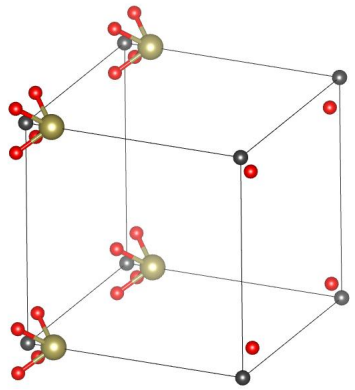

FIG. 3. $TeO_4$ unit cell p4mm symmetry.

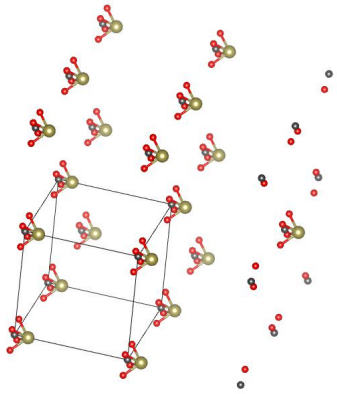

FIG. 4. $TeO_4$ $2 \times 2 \times 2$ supercell p4mm symmetry.

the lowest energy. Then the minimum energy of $2 \times 2 \times 2$ $O_2$ supercell is calculated by using the vc-relax scheme.

From energy values shown in IV, the formation energy of $TeO_2$ is calculated and found out to be:

$$E_{TeO2} - E_{Te+O2} = +6.053 Ry/atom$$

### D. Supercell construction, optimization and formation energy of $TeO_4$ and $Te(OH)_4$

The hypothetical molecular crystals $Te(OH)_4$ and $TeO_4$ were built using Vesta [14] and GaussView[19]. The distance between Te-O in $Te(OH)_4$ is 1.82496 Å[3], O-H bond length is 0.96002 Å[3] and the intramolecular hydrogen bonding distance was kept as 2.18099 Å. The unit cell was constructed with p1m1 symmetry and was optimized using vc-relax to find minimum energy. Supercell optimization was not carried out due to computational limitations. But the convergence test for supercells showed that 2×2×2 supercell had the lowest energy among 2×2×1, 2×1×2, 1×2×2, 1×1×2, 1×2×1 and 2×1×1 supercells. Similarly, $TeO_4$ molecular crystal was built and its unit cell was optimized. The optimization of these crystals were carried out with the help of SEAGrid [20] High Performance computers. A gaseous state calculation of $Te(OH)_4$ and $TeO_4$ was also done with GAMESS using Chemcompute [21] HPC. The energy of the gaseous state and the solid state was compared to realize its stability. To support this stability model, the formation energy of $Te(OH)_4$ was calculated. A similar procedure is implemented for $TeO_4$ .

The equilibrium energy of $TeO_4$ and $Te(OH)_4$ unit cell are -528.42193528 Ry and -533.90631695 Ry. The corresponding gaseous state equilibrium energy of $Te(OH)_4$ is -3436.075453 Ry. The structure of $TeO_4$ is unstable in gaseous state. The formation energy of $TeO_4$ was calculated by subtracting the equilibrium energy of $TeO_4$ from the equilibrium energy of Te unit cell and Oxygen supercell. The formation energy of $TeO_4$ was found to be +643.3504427 Ry/atom. A similar calculation is made for $Te(OH)_4$ with hydrogen supercell and the formation energy of $Te(OH)_4$ is found to be +44.86024652 Ry/atom.

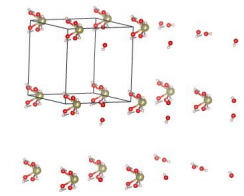

FIG. 5. $Te(OH)_4$ unit cell p1m1 symmetry.

## IV. DISCUSSION AND CONCLUSION

From the above results, it is evident that both solid and gaseous form of $Te(OH)_4$ are much more stable than the $TeO_4$. It is due to the intramolecular hydrogen bonding present in the $Te(OH)_4$, see the dashed bonds in figure, 5, 6 and 8. It stabilizes the neighbouring oxygen atoms. Whilst in the case of $TeO_4$, the coordination number is 8. The normal double bond length of oxygen is around 1.21 Å. Such a shorter distance between oxygen and this

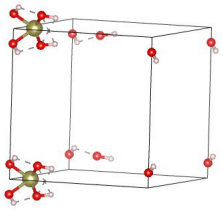

FIG. 6. $Te(OH)_4$ $2 \times 2 \times 2$ supercell p1m1 symmetry.

TABLE IV. Equilibrium energies for the crystals used for formation energy calculations obtained using Quantum Espresso.

| Crystal | Number of atoms per unit cell/supercell | Equilibrium Energy [Ry] |
|---|---|---|
| Te | 3 (unit cell) | -1087.820157 |
| $2 \times 2 \times 2$ $O_2$ supercell | 64 | -2657.35399 |
| $2 \times 2 \times 2$ $H_2$ supercell | 16 | -18.66991 |
| $TeO_2$ | 24 (unit cell) | -3566.89763 |
| $TeO_4$ | 5 (unit cell) | -528.42193 |
| $Te(OH)_4$ | 9 (unit cell) | -533.90631 |

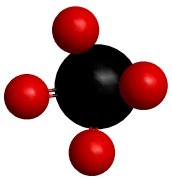

FIG. 7. Gaseous $TeO_4$.

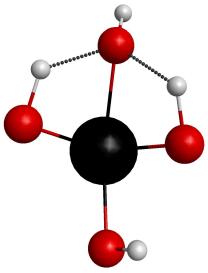

FIG. 8. Gaseous $Te(OH)_4$.

heavy atom may create an unstable environment. The formation energy of $TeO_4$=+ 643.3504427 Ry/atom is greater than that of $Te(OH)_4$=+44.86024652 Ry/atom. This shows a greater possibility towards the formation $Te(OH)_4$ than $TeO_4$. Furthermore, the stability of the highest oxidation state of the chalcogens decreases down the column. This causes destabilization of $TeO_4$.

Among the Chalcogens, Te and Po are the only two elements that has the tendency to form molecules at +8 oxidation state. These study reports on Te in +4 state and +8 state may pave a path for the Polonium crystal studies. There is fair chance that Polonium in +4 and +8 state may inherit the properties of similar Tellurium crystal systems.

## ACKNOWLEDGMENTS

The authors of this project would like to deeply thank prof. Stefaan Cottenier from Ghent University for his efforts to make the course available for everyone interested in computational materials sciences and the opportunity to work in this project from abroad and also thank Dr. Sudhakar Pamidighantam and the SEAGrid for providing the HPC access for the project.

[1] The nobel prize in physics 1903.
[2] Polonium.
[3] J. R. Rumble, Handbook of chemistry and physics (CRC Press, 2016) pp. 4–27.
[4] A. E. N.N. Greenwood, ed., Chemistry of the elements (Elsevier Ltd, 1997) pp. 747–788.
[5] Periodic table (2005).
[6] A. Jain, S. P. Ong, G. Hautier, W. Chen, W. D. Richards, S. Dacek, S. Cholia, D. Gunter, D. Skinner, G. Ceder, and K. a. Persson, The Materials Project: A materials

genome approach to accelerating materials innovation, APL Materials **1**, 011002 (2013).

[7] P. G. et al., Quantum espresso: a modular and open-source software project for quantum simulations of materials, Journal of Physics: Condensed Matter **21**, 395502 (19pp) (2009).

[8] P. G. et al., Advanced capabilities for materials modelling with quantum espresso, Journal of Physics: Condensed Matter **29**, 465901 (2017).

[9] J. P. Perdew, K. Burke, and M. Ernzerhof, Generalized gradient approximation made simple, Phys. Rev. Lett. **77**, 3865 (1996).

[10] M. Ernzerhof and G. E. Scuseria, Assessment of the perdew–burke–ernzerhof exchange-correlation functional, The Journal of Chemical Physics **110**, 5029 (1999), https://doi.org/10.1063/1.478401.

[11] B. et al., enRecent developments in the general atomic and molecular electronic structure system, The Journal of Chemical Physics **152**, 154102 (2020).

[12] F. Jensen, *Introduction to Computational Chemistry*, 3rd ed. (John Wiley Sons, 2017).

[13] T. Björkman, Cif2cell: Generating geometries for electronic structure programs., Comput. Phys. Commun. **182**, 1183 (2011).

[14] K. Momma and F. Izumi, *VESTA3* for three-dimensional visualization of crystal, volumetric and morphology data, Journal of Applied Crystallography **44**, 1272 (2011).

[15] D. H. H.T. Stokes and B. Campbell, Program for identifiying the space group symmetry of a crystal, J. Appl. Cryst. **38**, 237 (2005).

[16] D. H. H.T. Stokes and B. Campbell, Findsym, isotropy software suit, .

[17] F. Birch, Finite elastic strain of cubic crystals, Phys. Rev. **71**, 809 (1947).

[18] F. D. Murnaghan, The compressibility of media under extreme pressures, Proceedings of the National Academy of Sciences **30**, 244 (1944), https://www.pnas.org/content/30/9/244.full.pdf.

[19] R. Dennington, T. A. Keith, and J. M. Millam, Gaussview Version 6 (2019), semichem Inc. Shawnee Mission KS.

[20] S. Pamidighantam, S. Nakandala, E. Abeysinghe, C. Wimalasena, S. R. Yodage, S. Marru, and M. Pierce, Community science exemplars in seagrid science gateway: Apache airavata based implementation of advanced infrastructure, Procedia Computer Science **80**, 1927 (2016), international Conference on Computational Science 2016, ICCS 2016, 6-8 June 2016, San Diego, California, USA.

[21] B. et al., Recent developments in the general atomic and molecular electronic structure system, The Journal of Chemical Physics **152**, 154102 (2020), https://doi.org/10.1063/5.0005188.

[22] S. Pamidighantam, S. Nakandala, E. Abeysinghe, C. Wimalasena, S. R. Yodage, S. Marru, and M. Pierce, Community science exemplars in seagrid science gateway: Apache airavata based implementation of advanced infrastructure, Procedia Computer Science **80**, 1927 (2016), international Conference on Computational Science 2016, ICCS 2016, 6-8 June 2016, San Diego, California, USA.